

Hopping and diffusion of ultrasoft particles in cluster crystals in the explicit presence of a solvent

This article has been downloaded from IOPscience. Please scroll down to see the full text article.

2013 J. Phys.: Condens. Matter 25 195101

(<http://iopscience.iop.org/0953-8984/25/19/195101>)

View the [table of contents for this issue](#), or go to the [journal homepage](#) for more

Download details:

IP Address: 131.130.239.55

The article was downloaded on 05/04/2013 at 13:48

Please note that [terms and conditions apply](#).

Hopping and diffusion of ultrasoft particles in cluster crystals in the explicit presence of a solvent

Marta Montes-Saralegui¹, Arash Nikoubashman^{1,2} and Gerhard Kahl¹

¹ Institut für Theoretische Physik and Centre for Computational Materials Science (CMS), Technische Universität Wien, Wiedner Hauptstraße 8–10, A-1040 Wien, Austria

² Department of Chemical and Biological Engineering, Princeton University, Princeton, NJ 08544, USA

E-mail: marta.montes.saralegui@tuwien.ac.at

Received 24 January 2013, in final form 7 March 2013

Published 3 April 2013

Online at stacks.iop.org/JPhysCM/25/195101

Abstract

We have investigated diffusion and hopping processes in a cluster crystal formed from mesoscopic, ultrasoft particles. In contrast to previous contributions we have explicitly included in our investigations the microscopic solvent by using a simulation scheme that takes the induced hydrodynamic interactions into account as faithfully as possible. In our investigations we first focused on the processes of migration of the ultrasoft particles. By evaluating dynamical correlation functions we were able to demonstrate that the presence of the solvent does indeed have an important impact on the diffusion and hopping processes of the particles: this applies in particular to the diffusive behaviour, to the angular orientation of the jump events and to the spatial extents of these events. In a second set-up we have added non-cluster-forming ultrasoft particles to the system, investigating thus the impact of the solvent and that of the mutual interaction of the two species of ultrasoft particles on their respective dynamic behaviours. Our investigations clearly demonstrate, beside the expected significant role that the solvent plays in this set-up, that diffusion and the jump processes show distinct differences for the two particle species.

(Some figures may appear in colour only in the online journal)

1. Introduction

During recent years, systems of ultrasoft particles that are able to form stable clusters have provoked a considerable amount of interest in the field of soft matter physics [1–7]. Opposed to traditional cluster formers, where the aggregation of particles is the consequence of competing interparticle interactions operating on different length scales (see for example [8–11]) we consider in this contribution (colloidal) particles where the (effective) potentials is ultrasoft (i.e. bounded) and purely repulsive. The only necessary prerequisite for the stability of the emerging clusters is the existence of negative components in the Fourier spectrum of the interaction potential [3].

At low and intermediate densities and elevated temperatures these clusters are predominantly polydisperse in their size and form—along with isolated particles—a disordered

fluid phase. However, at sufficiently high densities and sufficiently low temperatures the clusters populate the lattice sites of an face-centred (fcc) or a body-centred (bcc) cubic lattice [1]. And finally, at very low temperatures the phase diagram provides evidence of very complicated transitions between ordered phases [7]. These cluster crystals show some unexpected features, such as density-*independent* lattice constants or a complex reaction scenario as pressure is exerted on the crystal [2]. The formation of stable ordered cluster phases by particles that interact exclusively via repulsive potentials is admittedly counterintuitive at first sight. In contrast to crystals formed by conventional systems (such as Lennard-Jones particles), the clusters of overlapping ultrasoft particles are stabilized entirely by the repulsion experienced from the neighbouring cluster sites: although the interactions are repulsive throughout, a tagged cluster only reluctantly

moves out of its equilibrium position, because the repulsion it feels from one of its neighbours is even stronger than in its original position. We refer the reader to figure 1 in [12] for a nice, simplistic and intuitive cartoon of a one-dimensional cluster crystal and the related discussion. Meanwhile their surprising properties are well understood [3–5].

At this point it should also be mentioned, that recently the quantum counterpart of such ultrasoft particles has received attention [13, 14]: among others, ‘an intriguing phase consisting of a crystal of mesoscopic superfluid droplets’ was identified for Bose soft discs in two dimensions.

In this contribution, we focus on a specific dynamic phenomenon occurring in cluster crystals, the so-called *particle hopping*: through thermal agitation, particles can—in principle—overcome the energy barrier separating neighbouring lattice sites [12] and ‘hop’ to an adjacent cluster. These jumps are not restricted to the nearest neighbours, and trajectories spanning over several lattice sites have been observed in simulations [15].

Several features of this hopping processes were investigated in detail by the means of molecular dynamics (MD), Monte Carlo (MC) and Brownian dynamics (BD) simulations [15–17]: it was found that particles propagate in a cluster crystal between lattice sites through an activated hopping mechanism [16, 17] and the question was raised whether the diffusive motion of the particles corresponds to anomalous diffusion [15], a feature that is typical for Lévy flights [18–21].

However, all the preceding studies did not accurately incorporate the effects of the solvent and the ensuing hydrodynamic interactions. Of course its influence can be considered to be of less relevance in investigations dedicated to the *static* properties, such as the phase diagram. However, as we proceed to *dynamic* properties, such as diffusion, the solvent often plays a significant role, and therefore should not (or even must not) be neglected in a faithful description of the system. The relevance of the solvent for the dynamics has been shown, for instance, for charged colloidal suspensions [22] and for short polymer chains [23]. We will demonstrate in this contribution that this is also the case for our system at hand.

In the present contribution we *explicitly* take into account the solvent and investigate its influence on hopping processes in cluster crystals. This is achieved by combining conventional molecular dynamics (MD) simulations for the solute particles with multi-particle collision dynamics (MPCD) simulations [24, 25]: in the latter concept alternating streaming and collision steps are performed, where the former ones describe the ballistic motion of the solvent particles, while the latter ones mimic the collision of the solvent with the solute particles.

In our investigations we have considered two set-ups: (I) In a first experiment we have investigated—similar as in [15]—the hopping process of the cluster-forming particles under the explicit presence of the solvent. We have inspected in detail the characteristic features of hopping processes (such as jump lengths and directional distributions of jump events), and of the dynamic properties (such as the mean-squared

displacement and the self-part of the van Hove correlation function). These results provide qualitative and quantitative evidence that the dynamics of hopping processes is drastically reduced with increasing influence of the solvent. In addition, analysing characteristic features of the migrating particles gives an unambiguous answer, that for a finite coupling between the solute particles and the solvent, this hopping process does *not* show any sub-diffusive behaviour; in view of the fact that MPCD simulations feature a more realistic dynamics (than the Newtonian MD simulations), we can conclude that in experimental system a Lévy flight type behaviour can definitely be excluded. (II) In a second experiment we have added non-cluster-forming colloidal particles to a cluster crystal and have re-investigated the hopping process of both types of colloidal particles under the influence of the solvent. As already known from the MD-based investigations presented in [17] (where the solvent was neglected) we find that the dynamic scenario encountered in this system is the result of the complex interplay of the dynamics of the cluster-forming fluid particles and the non-cluster-forming particles. In addition, we are able to show that a faithful description of the solvent drastically influences the dynamics of both types of solute particles.

The rest of this paper is structured as follows: in section 2 we present the two set-ups investigated in this contribution and briefly summarize our simulation technique. Results are compiled and discussed in section 3 and the paper is closed by a summary.

2. Model and simulation method

2.1. The model

In our investigations we have considered cluster crystals, where the lattice positions are occupied by clusters of overlapping, ultrasoft (mesoscopic) particles. This crystal is assumed to be in contact with a (microscopic) solvent. The solute particles interact via the GEM- n potential, $\Phi_n(r)$, given by:

$$\Phi_n(r) = \epsilon \exp [-(r/\sigma)^n], \quad (1)$$

with ϵ and σ being the energy- and length units, respectively. The mass of these particles is defined as m and will be specified further below. As shown in [26], particles interacting through the potential specified in equation (1) are able to form stable clusters only if $n > 2$.

As outlined in the introduction, we *first* consider an fcc cluster crystal where particles interact via a GEM-4 potential in the explicit presence of a microscopic solvent (henceforward referred to as Case I). The particular choice for the potential index was motivated by the fact that the phase diagram for $n = 4$ is known in detail [1, 3, 4, 7]. In addition, the only study dedicated to hopping processes in ultrasoft cluster crystals published so far has been carried out for this particular potential parameter [15].

In the *second* experimental set-up (henceforward referred to as Case II), we have added to this system *non-cluster-forming* particles (referred to as type-A particles). For these

Table 1. System parameters of all investigated systems (Cases I and II, as specified): concentration of the cluster-forming type-B particles, c_B (only Case II), lattice constant of the cluster crystal, a (in units of σ), simulation box size L (in units of σ), and average cluster size $\langle N_c \rangle$.

	c_B	a	L	$\langle N_c \rangle$
Case I		2.018	8.073	13.15
Case II	0.65	1.930	7.718	7.57
	0.80	1.896	7.584	8.73
	0.95	1.864	7.456	9.76
	1.00	1.857	7.428	10.25

investigations we have chosen $n = 8$ for the interaction between the cluster-forming particles (type-B particles). The choice for this potential parameter is motivated by the investigations presented in [17] and is justified by the fact that the change from $n = 4$ (Case I) to $n = 8$ (Case II) will affect the properties of the cluster crystal only on a *quantitative* but not on a *qualitative* level. The additional mesoscopic particles interact via a GEM-2 potential, guaranteeing that these particles definitely will not form stable clusters [26]. For the cross interaction between the two types of ultrasoft particles we have assumed—similar as in [17]—a GEM-4 potential, i.e., an interaction that also supports cluster formation. The interaction potential for the second set-up is given by the equation (1), introducing the type-dependent parameters $\sigma_{AA} = 0.3\sigma$, $\sigma_{AB} = 0.6\sigma$, and $\sigma_{BB} = \sigma = 1$, as well as $n_{AA} = 2$, $n_{AB} = 4$, and $n_{BB} = 8$.

The parameters of the systems treated in the two set-ups are specified in table 1.

2.2. The simulation method

For our investigations we have used the MPCD simulation technique [24, 25], i.e. a mesoscopic, particle-based simulation method that takes hydrodynamic interactions (HI), which are induced by the solvent, into account as faithfully as computationally feasible. Being a hybrid simulation approach, the solute–solute interactions are treated in a standard MD simulation, while the influence of the solvent is incorporated through alternating streaming and collision steps. The solvent particles are assumed to be non-interacting and propagate ballistically in the simulation box during the streaming steps. Thus the position of the i th solvent particle at the next time step $t + \Delta t$, $\mathbf{r}_i(t + \Delta t)$, is simply given by:

$$\mathbf{r}_i(t + \Delta t) = \mathbf{r}_i(t) + \Delta t \mathbf{v}_i(t), \quad (2)$$

with \mathbf{v}_i being its velocity. For the collision step, the solvent particles are first sorted into cubic cells of edge length c , a value which determines the spatial resolution of the HI. For our simulations we have chosen $c = \sigma$ in order to fully capture the HI between the lattice sites. Introducing the centre of mass velocity of the j -th cell (to which the i -th solvent particle belongs), $\mathbf{u}_j(t)$, the velocities $\mathbf{v}_i(t)$ are calculated according to the following law:

$$\mathbf{v}_i(t + \Delta t) = \mathbf{u}_j(t) + \Omega(\alpha) [\mathbf{v}_i(t) - \mathbf{u}_j(t)]. \quad (3)$$

In the above relation, $\Omega(\alpha)$ is a norm-conserving rotation matrix around a fixed angle α around a randomly chosen unit vector [27]. It can be shown that the dynamics defined by the above two equations preserves total energy and momentum in each cell and consequently in the entire system. The mean free path of a solvent particle, λ , is then given by $\lambda \sim \Delta t \sqrt{T}$ and it has been shown in [28] that Galilean invariance is violated for $\lambda < c/2$. Therefore, all cells are shifted by a randomly chosen vector, whose components are drawn from the interval $[-c/2, +c/2]$ before each collision step.

The interaction between solvent and solute particles is modelled by including the solute particles in the collision step. In this way, solute and solvent particles exchange momenta. In order to maintain a constant temperature T in our simulations we rescaled the relative velocity components by a scaling factor, which adjusts the total kinetic energy to the desired value [24]. In the MPCD simulations, this procedure was only applied to the *solvent* particles, and in this scheme the solvent can be considered as a heat bath for the *solute* particles. In the MD simulations, we directly rescaled the velocities of the GEM particles during the initial equilibration (5×10^6 timesteps). Once the system reached its steady state, we deactivated the thermostat and verified that the temperature of the system remained constant.

We have set the mass m' of the solvent particles to unity, and filled each collision cell with 30 solvent particles. The mass of the GEM particles was then set to $m = 6$, and the collision angle α to 130° . Our unit of time is thus given by $\tau^* = \sqrt{m' \sigma^2 / \epsilon}$, and the time step for the MD algorithm was set to $\Delta t_{MD} = 0.002$. An MPCD step was performed after each τ MD steps, so that $\Delta t = \tau \Delta t_{MD}$. In order to study the influence of the HI, different values of τ have been chosen, which will be specified in section 3. It should be noted that for $\tau \rightarrow \infty$, the simulation technique becomes identical to conventional MD simulations. Each simulation was run for a total time of $t_{total} = 10000\tau^*$, and during the run, positions and velocities of the colloidal particles have been recorded.

Based on these quantities, dynamic correlation functions have been evaluated in a post-processing routine. To be more specific we have calculated from the particle positions:

- (i) The mean-squared displacement, $\delta r_i^2(t)$, defined as:

$$\delta r_i^2(t) = \langle |\mathbf{r}_i(t) - \mathbf{r}_i(0)|^2 \rangle. \quad (4)$$

From its time dependence, one can draw conclusions whether the particles propagate (predominantly) ballistically, or if they show diffusive behaviour (be it either sub-diffusive or normal).

- (ii) The self-part of the van Hove correlation function, given by:

$$G_s(r, t) = \left\langle \frac{1}{N} \sum_{i=1}^N \delta[r - |\mathbf{r}_i(t) - \mathbf{r}_i(0)|] \right\rangle. \quad (5)$$

This function correlates the position of a tagged particle (with index i) at time $t = 0$ with its location at some time $t > 0$. It thus provides information about the spatio-temporal correlations of a particle [29, 30].

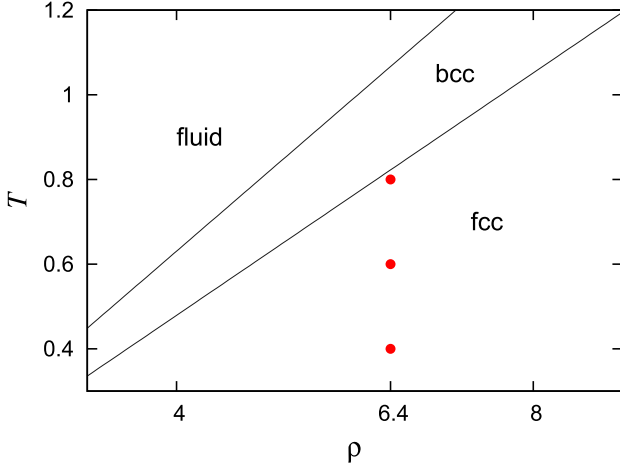


Figure 1. Schematic phase diagram of a system of GEM-4 particles in the (T, ρ) -plane, indicating the range of stability of the fluid phase and of the bcc- and fcc cluster phases. Filled circles specify cluster systems investigated in this contribution.

3. Results

3.1. Case I—cluster crystals in the presence of an explicit solvent

The state points that we have investigated for this particular set-up are specified in figure 1, and it is clearly visible that all the investigated state points correspond to cluster crystals. The influence of the solvent properties (and the ensuing impact of HI) was systematically investigated by varying the value of τ (specified in section 2.2).

We start our discussions of the results with the mean-squared displacement, as defined in equation (4). Figure 2 shows $\delta r^2(t)$, i.e. the average taken over all solute particles as a function of time t , for three different temperatures ($T = 0.8, 0.6$, and 0.4). For each temperature, different τ -values have been considered (as specified in the figures). According to the evolution of $\delta r^2(t)$, four different time regimes can be identified: the (trivial) ballistic regime at small t -values, followed by a region where $\delta r^2(t)$ shows oscillations, then a plateau-like region, and finally the long-time regime, corresponding to normal diffusion. Depending on the combinations of the T - and τ -values, some of the regimes are covered by or are merged with other regimes.

At high temperatures, we observe for vanishing and weak HI (i.e. $\tau \gtrsim 250$) characteristic high-frequency oscillations due to single particle vibrational modes of the particles within their clusters. With increasing influence of the solvent, these oscillations are gradually suppressed, leading to a plateau that extends approximately over one decade in time. This behaviour is due to the fact that for small τ -values the particles collide more frequently with the surrounding solvent particles and thus quickly lose their memory about their original flight direction, i.e. effects of inertia become completely negligible. For larger t -values, the thermal energy (which is now of the order of magnitude of the energy barrier between two clusters) allows solute particles to spontaneously jump from

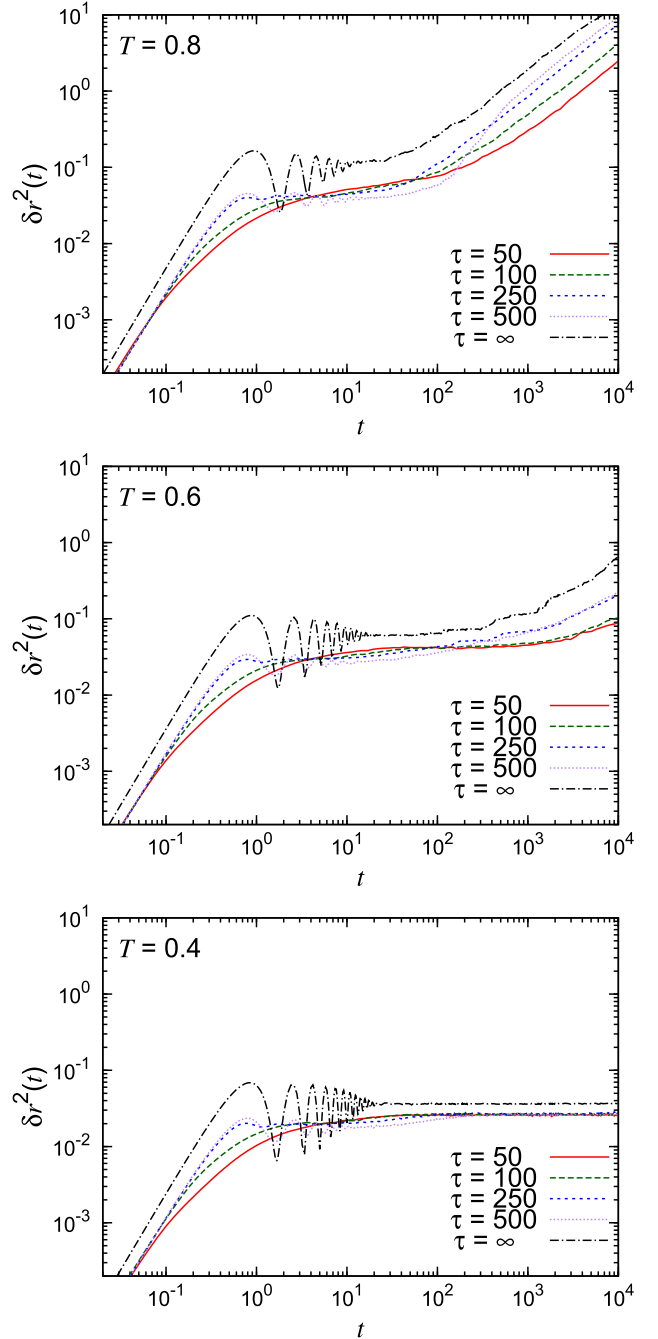


Figure 2. Mean-squared displacement, $\delta r^2(t)$, as a function of time t for three different temperatures as labelled for a system of cluster-forming GEM-4 particles in the presence of a solvent. The black (dash-dotted) curve displays MD simulation results (corresponding to $\tau = \infty$). The other curves correspond to data obtained in MPCD simulations with $\tau = 50, 100, 250$, and 500 , respectively, as labelled.

their original cluster to a neighbouring lattice site, leading to normal diffusion at large timescales. In this regime, the actual value of the diffusion constant depends strongly on the solvent: over the τ -range considered in this contribution this quantity differs by one order of magnitude and attains its highest value in the complete absence of the solvent, i.e. for Newtonian dynamics realized in MD simulations.

As the temperature is decreased, the high-frequency modes show the same τ -dependence as those observed for $T = 0.8$; they are slightly more pronounced and extend over a significantly larger time regime. The decreasing temperature has a distinct influence on the long-time behaviour of the mean-squared displacement: with decreasing temperature the plateau region continuously extends with decreasing temperature over a larger time span. At the lowest temperature considered ($T = 0.4$), the curves of the mean-squared displacement remain flat (i.e. the diffusion constant vanishes) over the observed time range. This is a consequence of the fact that the very small thermal agitations essentially suppress any particle exchange between lattice sites (see quantitative discussion below).

In an effort to obtain a better understanding of the diffusive behaviour of the solute particles we have analysed the individual hopping processes of particles between clusters in more detail. To this end a few definitions are in order:

- (i) Using the same algorithm to identify clusters as the one put forward in the appendix of [15], we have recorded the trajectories of all particles along the simulation runs in terms of jump events.
- (ii) A jump event starts as a tagged particle leaves its (donor) cluster (located at the centre of mass of the initial cluster, \mathbf{R}_i^{CM}) and terminates when it stays in a target (acceptor) cluster (located at the centre of mass of the target cluster, \mathbf{R}_t^{CM}) over a time span longer than a specified residual time, t_{res}^* . For our simulations we have chosen $t_{\text{res}}^* = 2$, i.e. a time span which is of the order of a few vibrational modes (see figure 2). We have verified that different choices for the value of t_{res}^* (for instance, $t_{\text{res}}^* = 3$ or 4) have no quantitative influence on the results. Three different types of hopping events can be identified: (a) the jump event starts and terminates at the same cluster; (b) the particle hops directly from its initial to the final target cluster; and (c) the particle passes along its trajectory at some intermediate clusters.
- (iii) We define the net jump length as $r_{\text{net}} = |\mathbf{R}_t^{\text{CM}} - \mathbf{R}_i^{\text{CM}}|$. The possible consecutive jumps within the unit cell of the fcc cluster crystal are illustrated in figure 7 of [15]. Since the jumps occur between lattice sites, all distances can conveniently be expressed in units of the nearest neighbour distance in an fcc crystal, $d_{\text{nn}} = a/\sqrt{2}$, with a being the lattice constant of the cubic fcc unit cell.

In figure 3 we have depicted the net jump length distribution, $P_{\text{net}}(r/d_{\text{nn}})$, as a function of r for selected τ -values and for two temperatures, namely $T = 0.8$ and 0.6 . At $T = 0.4$, essentially no jump events could be identified; this observation correlates nicely with the curves for the mean-squared displacement which are completely flat at this low temperature, i.e. no diffusion takes place at all. In contrast, for the higher temperatures (i.e. $T = 0.6$ and 0.8), the peaks in $P_{\text{net}}(r)$ (cf figure 3) and the linear increase in the mean-squared displacement (reflecting a diffusive behaviour of the particles; cf figure 2) provide a consistent picture that particle hopping is the dominant mass transport

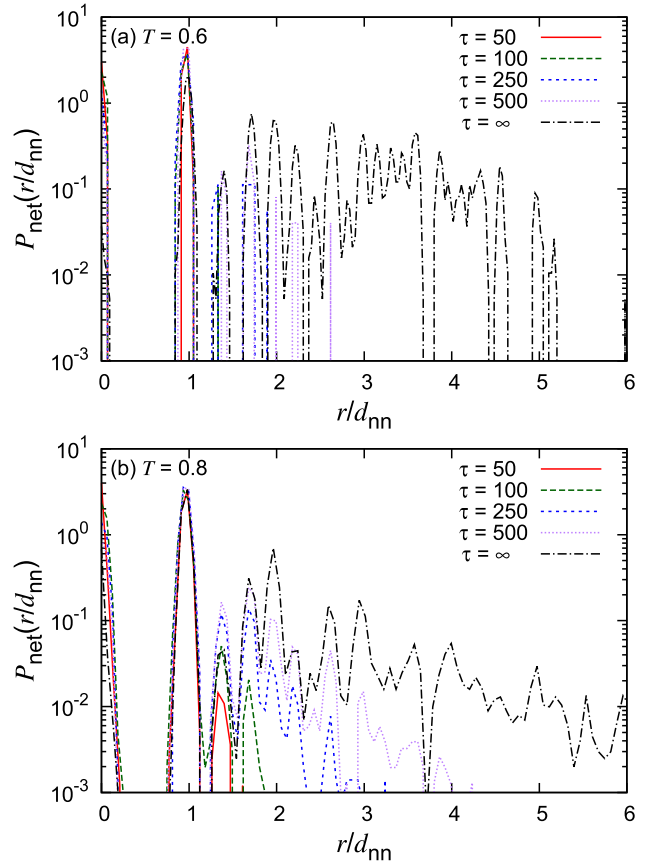


Figure 3. Net jump length distribution $P_{\text{net}}(r/d_{\text{nn}})$ as a function of r/d_{nn} for $T = 0.6$ and 0.8 and selected τ -values as indicated for a system of cluster-forming GEM-4 particles in the presence of a solvent on a semi-logarithmic scale. The black (dash-dotted) curve displays MD simulation results (corresponding to $\tau = \infty$). The other curves correspond to the MPCD simulations with $\tau = 50$, 100 , 250 and 500 respectively as labelled.

mechanism in cluster crystals. From the data presented in figure 3 we can make the following two conclusions: first, the jump length increases as the temperature grows. Second, the surrounding solvent plays a crucial role in the jump events of the GEM particles: for small τ -values and consequently for small values of the mean free path length, λ , the distribution functions $P_{\text{net}}(r/d_{\text{nn}})$ show distinct peaks at the positions of the nearest neighbour clusters but decay rapidly with growing distance. In contrast, pure MD simulations lead to distribution functions that display peaks of sizeable height at even larger distances (corresponding to integer multiples of d_{nn}), suggesting preferred straight hopping trajectories through the cluster crystal. These conclusions on the impact of the solvent on the jump events become even more evident from selected numerical data for the maximum net jump length, r_{max} (compiled in table 2), which can be up to a factor of 20 larger when the solvent is ignored. A final remark on the pronounced peak of $P_{\text{net}}(r/d_{\text{nn}})$ at $r = 0$ is in order: this feature corresponds to type-(a) jump events specified above in item (ii). Integrating over the corresponding peaks of $P_{\text{net}}(r/d_{\text{nn}})$ at $T = 0.8$ (which are hardly visible in figure 3) leads to data that are visualized in figure 4: for strong solute–solvent coupling (i.e., $\tau = 50$) nearly all jump

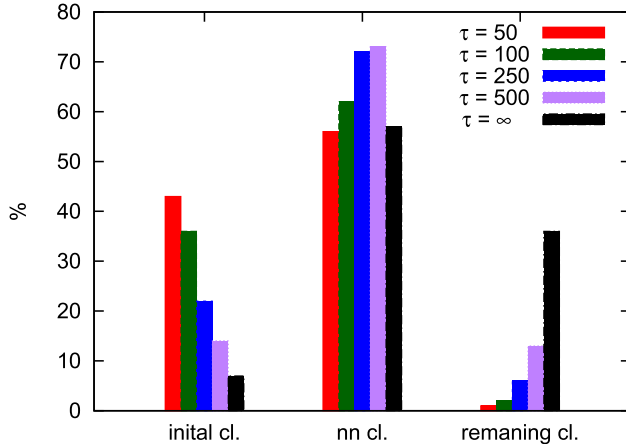


Figure 4. Integrated values of the net jump length distribution, $P_{\text{net}}(r/d_{\text{nn}})$ (cf figure 3), integrated over distances corresponding to the initial cluster ('initial cl.'), the nearest neighbour clusters ('nn cl.') and the remaining clusters ('remaining cl.') in per cent for different τ -values as labelled.

Table 2. Largest net jump length, r_{\max}/d_{nn} , for two selected temperatures (i.e. $T = 0.6$ and 0.8) and for selected τ -values.

τ	$T = 0.6$	$T = 0.8$
50	1.0	1.4
100	1.3	2.2
250	1.9	3.6
500	2.6	5.0
∞	6.0	28.0

events are restricted to the cluster of origin (43%) and to the clusters in the nearest neighbour shell (56%); only very few particle trajectories (1% or even less) end in clusters that are further away. In contrast, in the complete absence of solute–solvent coupling (i.e., $\tau = \infty$) only a few jump events terminate in the cluster of origin (some 7%) while a sizeable number of particle trajectories extend even beyond the nearest neighbour distance (some 36%). Thus a strong coupling between the solute particles and the solvent seems to introduce an additional energetic barrier which prevents solvent particles to escape from their cluster of origin.

Finally, from the data presented in figure 3 we can definitely exclude the occurrence of Lévy flights in cluster crystals in the presence of an explicit solvent: as in figure 5 of [15], $P_{\text{net}}(r)$ shows in the absence of the solvent (i.e. in MD simulations) a power law decay, i.e., $\sim 1/r^{1+\alpha}$, with $\alpha \sim 2.2$ [15], which represents an α -value which is slightly larger than the upper limit required for Lévy flights [18–21]. Increasing the influence of the solvent by decreasing τ we observe that the long-distance decay of $P_{\text{net}}(r)$ is characterized by increasingly larger α -values.

To further characterize the nature of the long range jumps in the cluster crystal we have extracted from our simulation data the correlation between the net jump length, r_{net} , and the angle Θ , enclosed by two successive segments of the trajectory of a jump event (for a visualization see figure 5). To this end we have considered all the type-(c) jump events specified above in item (ii) where the tagged

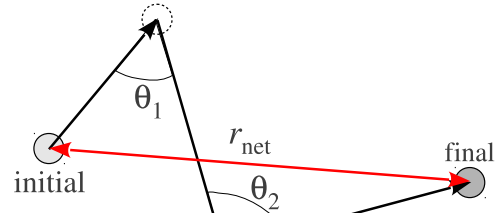


Figure 5. Schematic sketch of a jump event, visualizing the net jump length, r_{net} and the related angles Θ_1 and Θ_2 .

particle reaches its target cluster after several intermediate clusters. The resulting correlation is depicted in figure 6 for two different τ -values (i.e., $\tau = 50$ and ∞) at $T = 0.8$. The results for $T = 0.6$ are on a qualitative level comparable to the latter case, but less pronounced. Each grey symbol represents the aforementioned angle Θ identified along the trajectory of a jump event that extends over a net jump length of distance r/d_{nn} . The filled symbols represent the average Θ -value at a given jump length r/d_{nn} . In the explicit presence of a solvent, the majority of jumps are rather short ranged. The preferred Θ -values are $\Theta = 0^\circ, 60^\circ$ and 90° , as the particles only jump back and forth to their second nearest neighbours, but do not move along straight trajectories through the crystal. This picture changes completely, when the HI are neglected: especially for longer jump lengths, Θ -values of 120° and 180° dominate, corresponding to slightly deflected or perfectly straight pathways through the crystal. Thus, the incorporation of HI significantly modifies the diffusion behaviour both on a qualitative as well as on a quantitative level: while in the MD simulations, the diffusion is dominated by long ranged and strongly correlated ballistic flights, the explicit presence of a solvent reduces the responsible mechanism for mass transport to random jumps on nearby lattice sites.

Finally, we have studied the influence of the properties of the solvent on time-dependent correlations functions through the self-part of the van Hove correlation function, defined in equation (5). The results for $G_s(r, t = 6000)$, evaluated at $T = 0.8$, are depicted in figure 7. For all τ -values considered in this contribution we observe cascades of peaks (with two pronounced peaks at $r = 0$ and d_{nn}). In contrast, the exponential decay at large distances depends in a highly sensitive way on τ : smaller τ -values (and therefore smaller mean free paths) lead to a faster decay, meaning that the hopping processes are limited to shorter jump lengths. For completeness we mention that for none of the τ -values and time ranges investigated in this contribution, a Gaussian shape for the self-part of the van Hove correlation function has been observed [29, 30]; however, we expect to observe this behaviour at considerably larger t -values.

3.2. Case II—cluster crystal and ultrasoft particles in the explicit presence of a solvent

Now that the migration of cluster-forming particles through cluster crystals in the explicit presence of a solvent is better

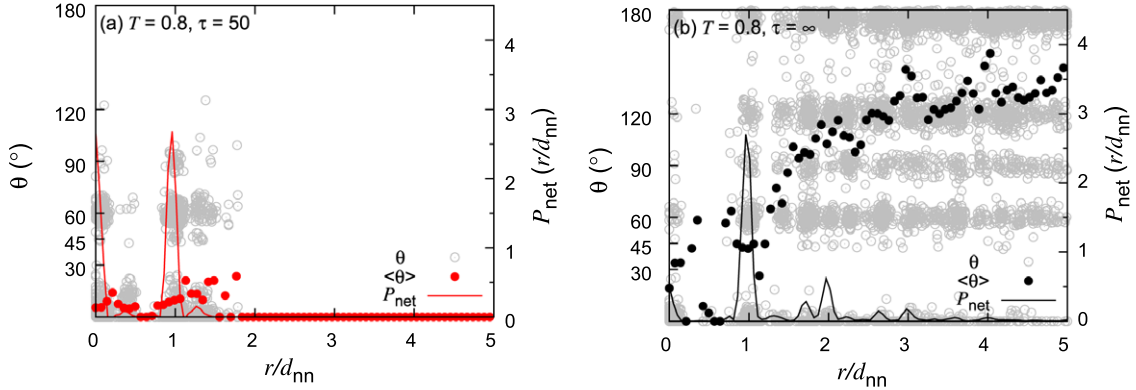


Figure 6. Correlation between the angle Θ and the net jump length r_{net} of a jump event (both quantities as specified in the text) as a function of r/d_{nn} at $T = 0.8$ for $\tau = 50$ (panel (a)) and $\tau = \infty$ (panel (b)) for a system of cluster-forming GEM-4 particles in the presence of a solvent. The solid line corresponds to the net jump length distribution $P_{\text{net}}(r/d_{\text{nn}})$ —cf figure 3. Open grey circles represent Θ -values identified in the trajectory of a jump event that extends over a net jump length of r/d_{nn} , filled circles correspond to the average of all Θ -values at a fixed jump length, denoted by $\langle \Theta \rangle$.

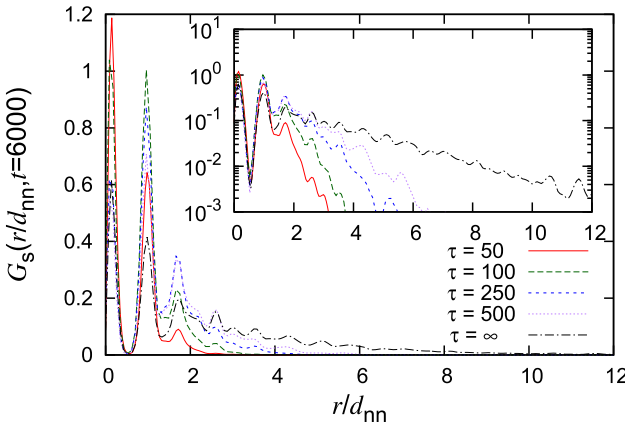


Figure 7. Main panel: self-part of the van Hove correlation function, $G_s(r, t)$, at $t = 6000$ as a function of r/d_{nn} at $T = 0.8$ for a system of cluster-forming GEM-4 particles. Results were obtained via MD (black) and MPCD simulations with $\tau = 50$ (red), 100 (green), 250 (blue) and 500 (purple). The inset shows the same data on a semi-logarithmic scale.

understood, we consider a more complex scenario in what follows: we add ultrasoft, *non-cluster-forming* particles to the set-up considered in section 3.1. In the following, we will denote these particles as type-A particles, while the cluster-forming particles will be specified by the label B (introducing their concentration, c_B). Using again the MPCD simulation scheme we study the dynamic behaviour of both types of ultrasoft particles.

In an effort to establish a relation with the results obtained recently for binary cluster crystals [17], we consider in the following a cluster crystal formed by GEM-8 particles, adding non-cluster-forming GEM-2 particles; the cross interaction between the two particle species is specified by an exponent $n = 4$ (cf equation (1)). The state points that have been investigated for this particular set-up are specified in table 1, and were taken from the above mentioned, previous work carried out for this very system (cf table 1 in [17]). As argued in this contribution on the basis of a simple mean

field approximation [31, 32], the corresponding states are selected to be located on the so-called λ -line, i.e., where the system is prone to crystallize. MD and MPCD simulations have been performed for three different temperatures, i.e. $T = 0.4, 0.6$, and 0.8 . For simplicity we have assumed only one τ -value, namely $\tau = 50$. Since the results for all three temperatures are on a qualitative level comparable, we focus in the following on $T = 0.8$, where the observed phenomena are most pronounced: with decreasing temperature (and the ensuing reduced thermal agitations) the hopping processes become less frequent.

In figure 8 we present the mean-squared displacement for the non-cluster-forming GEM-2 (type-A) particles, $\delta r_A^2(t)$, and of the cluster-forming GEM-8 (type-B) particles, $\delta r_B^2(t)$, as functions of time and for different values of c_B as obtained from the simulations.

A first, qualitative analysis of the mean-squared displacement of the type-A (GEM-2) particles, $\delta r_A^2(t)$, shown in figure 8(a) reveals the expected and rather rapid cross-over from the short-time ballistic motion to the long-time diffusive behaviour; the fact that—irrespective of the concentration c_B and the simulation scheme—all $\delta r_A^2(t)$ -curves are characterized in their long-time limit by the same slope provides evidence that the diffusion constant has in all cases the same value. Thus the cluster crystal has essentially no impact on the diffusion constant of the mobile particles. Further, in none of the curves an intermediate oscillatory region is observed, indicating that the A-particles behave as a fluid confined in a crystalline matrix of clustered B-particles. Throughout, a higher concentration in B-particles delays the onset of the diffusive behaviour: obviously due to the increase in the number of B-type particles, the interstitial, non-cluster-forming type-A particles experience through the GEM-4 cross interaction stronger bonds to the clusters which delay the diffusion and thus slow down the dynamics. Considering now the results of each type of the simulation schemes separately, we observe distinctive differences: in the MD simulations we see a rather direct and slightly concentration-dependent transition from the ballistic to the

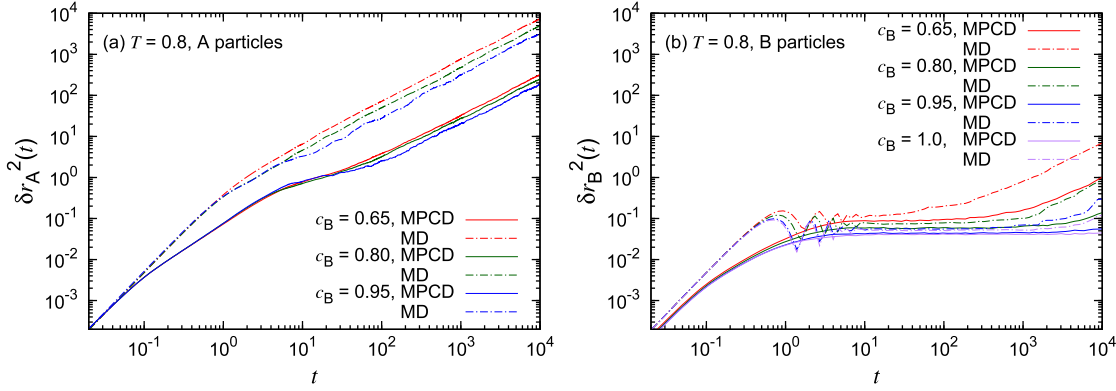


Figure 8. Mean-squared displacements, $\delta r_A^2(t)$ (panel (a)) and $\delta r_B^2(t)$ (panel (b)), as functions of t for $T = 0.8$ for a system of cluster-forming GEM-8 particles in the presence of non-cluster-forming GEM-2 particles and of a solvent. Dot-dashed lines correspond to the MD simulation results, while solid lines display MPCD data. Different colours correspond to different values of c_B (as labelled).

diffusive regime. In the MPCD simulations on the other hand, the ballistic behaviour terminates at $t \sim 10^{-1}$, followed by an intermediate regime that extends roughly over three time decades and is characterized by an exponent of approximately 1.25–1.3; eventually at $t \sim 10^2$ the diffusive behaviour sets in (see also the discussion of $G_s^A(r, t)$ below). The fact that in the explicit presence of the solvent the onset of the diffusive behaviour is delayed by two orders of magnitude with respect to the MD simulation data emphasizes the eminent role of the solvent.

For the type-B (GEM-8) particles we observe a similar time dependence of $\delta r_B^2(t)$ as the one observed for the pure GEM-4 case (cf section 3.1 and figure 2): the MD-data for $\delta r_B^2(t)$ show—after the ballistic regime—pronounced oscillations for all concentrations investigated, reflecting single particle vibrational modes of the particles in the clusters; eventually—and strongly dependent on c_B —the linear diffusive behaviour sets in. The fact that the onset of the diffusive regime shifts with increasing concentration of type-B particles to larger times is related to the fact that cluster crystals with higher c_B -values are characterized by larger occupancy numbers (see table 1); these larger clusters exert stronger binding forces on the mobile cluster-forming type-B particles and thus delay their diffusive behaviour. In the MPCD simulations, these oscillations are essentially suppressed due to the presence of the solvent. Instead we find a broad time regime where $\delta r_B^2(t)$ is essentially constant. Only towards the end of the investigated time range (i.e., $t \sim 10^4$), a c_B -dependent onset of the linear behaviour can be observed: the smaller c_B , the earlier the diffusive behaviour sets in (see also the related discussion in the previous paragraph).

Finally, we have evaluated the self-part of the van Hove correlation functions, $G_s^A(r, t)$ and $G_s^B(r, t)$, for different values of concentration c_B and different values of time t ; throughout, T was set to 0.8. The respective results are plotted in figure 9. By comparing the data presented in panels (a) and (b), we can trace how $G_s^A(r, t)$ develops at relatively short times: for very small t -values (i.e., $t = 80$), a strong correlation between the non-clustering type-A particles and the solvent particles can be observed, reflected in the MPCD data in well-defined peaks for $r \sim d_{nn}$, which

emerge for all concentrations; at $t = 800$, these peaks are smeared out over larger distances, but are still sizeable. In contrast, the MD simulation results for $G_s^A(r, t = 80)$ show no particular structure, indicating the rapid loss of spatio-temporal correlations of the A-type particles and at $t = 800$ this function has essentially vanished. This distinct difference emphasizes the eminent role of the solvent in supporting spatio-temporal correlations between the mobile, non-cluster-forming type-A particles over relatively large time spans. This phenomenon is also reflected by the intermediate region observed in $\delta r_A^2(t)$ for $10^{-1} \lesssim t \lesssim 10^2$ discussed above. Concluding we note that the loss of spatio-temporal correlations is fully confirmed by the Gaussian shape of $G_s^A(r, t)$ [29, 30]; the diffusion constants, that we obtain from the respective fits are in satisfactory agreement with the respective values extracted from the mean-squared displacements.

Finally, $G_s^B(r, t)$, is displayed in panels (c) and (d) of figure 9 for $t = 6000$. Within the MPCD simulation scheme, this function shows for all values of c_B pronounced peaks at $r \sim 0$ and $r \sim d_{nn}$ and then vanishes rapidly for larger distances, providing evidence that the solvent significantly slows down the mobility of the cluster-forming particles. In contrast, in the absence of the solvent well-defined peaks up to $r \sim 3d_{nn}$ are visible in the corresponding data of the MD simulations. In both cases, a strong c_B -dependence in the heights of the peaks is visible.

4. Conclusions

We have investigated the diffusion and the hopping processes that occur in a cluster crystal formed by mesoscopic, ultrasoft particles. These events are the result of the complex interplay of the thermal fluctuations and the coupling strength between the ultrasoft solute particles and the microscopic solvent: (i) if the thermal fluctuations are strong enough, the particles are (in principle) able to overcome the energetic barriers that separate the clusters from each other; (ii) however, in addition, these migration processes can be both fostered or hindered by the surrounding solvent.

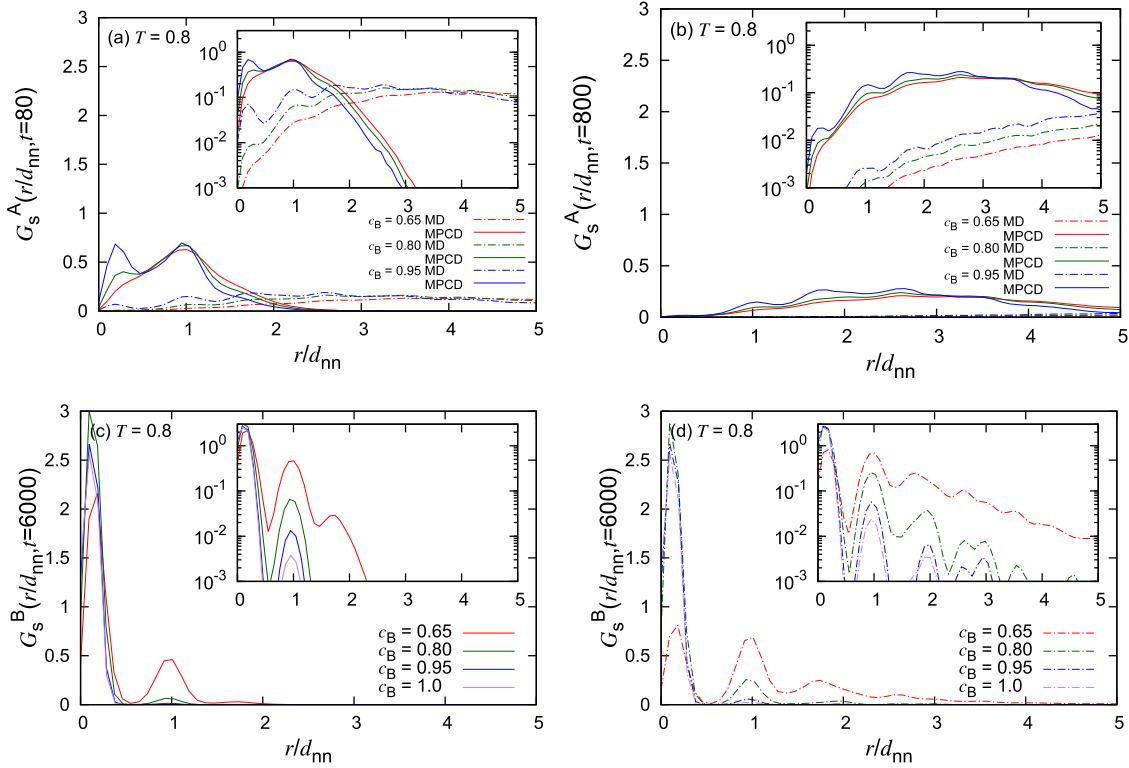


Figure 9. Self-part of the van Hove correlation functions $G_s^A(r, t)$ and $G_s^B(r, t)$ as functions of r/d_{nn} for $T = 0.8$, for a system of cluster-forming GEM-8 particles in the presence of non-cluster-forming GEM-2 particles and of a solvent. Panels (a) and (b): results for $G_s^A(r, t)$ for t -values as specified, as obtained by MD and MPCD simulations. Panels (c) and (d): $G_s^B(r, t)$ results for $t = 6000$, obtained by MPCD and MD simulations, respectively. Throughout, solid lines correspond to MPCD simulations and dashed-dotted lines to MD simulations. Different colours correspond to different values of c_B (as labelled).

In contrast to previous contributions, we have for the first time explicitly included the solvent (and the ensuing hydrodynamic interactions) in our investigations on the diffusion and hopping events in ultrasoft cluster crystals, and have thereby elucidated the eminent role of this medium in these processes. With the use of multi-particle collision dynamics we have employed a simulation scheme that takes these hydrodynamic interactions into account as faithfully as possible. In addition we can tune via a suitable parameter the coupling strength between the solvent and the solute particles. From the positions of the solvent particles, we analysed their trajectories in terms of their spatial extent and their directional distribution. Additional insight into these processes comes from the dynamic correlation functions: the mean-squared displacement gives evidence about the type of the occurring diffusion processes while the self-part of the van Hove correlation functions provides information about the spatio-temporal correlations of the solute particles.

In a first set-up we have studied the diffusion and hopping processes of a single species of ultrasoft cluster-forming particles in the explicit presence of a solvent. From the mean-squared displacement we learn that the solvent considerably delays the transition from the ballistic to the diffusive motion of the particles and essentially completely suppresses the inner-cluster vibrations of the particles; thus the solvent behaves as a damping buffer surrounding the clusters. Consequently, the hopping events of particles from

one cluster to a neighbouring one differ substantially from the case where no solvent is considered: the majority of jump events are either forth-and-back jumps to the initial cluster or, at most, to one of the neighbouring aggregates. Thus, the directional analysis of the trajectories shows that the vast majority of Θ -values lies between 0° and 90° ; in contrast, a related analysis for systems where the solvent is neglected leads to a broad spectrum of angles, with a strong dominance of straight or slightly deflected trajectories. Complementing a yet open question, we can definitely exclude through our analysis the occurrence of anomalous diffusion in cluster crystals.

In a second set-up we have added to the previous scenario non-cluster forming, mesoscopic particles as a minority component, denoted as type-A particles (in the presence of a cluster crystal formed by type-B particles); this scenario allows us to investigate both the influence of the solvent as well as of the mutual interaction between the two particle species on the migration of the solute particles. The mean-squared displacement of the type-A particles shows a novel diffusion behaviour, which is located between the ballistic and the diffusive regime and can be specified by a $\sim t^\xi$ power law, with $\xi = 1.25\text{--}1.30$. While the cluster crystal itself has no impact on the diffusive behaviour of the type-A particles, a larger concentration of type-B particles delays progressively the onset of the diffusive regime of the former due to the increasing strength of the cross interaction. But also

the onset of the diffusive behaviour of the cluster-forming type-B particles is increasingly delayed when increasing their concentration, due to the ensuing larger occupancy numbers of the clusters, which exert a stronger attraction to the migrating particles. From the self-part of the van Hove correlation functions we learn that the spatio-temporal correlations of the two particle species are influenced in a distinctively different way by the solvent. For the type-A particles the strong spatio-temporal correlations are mediated via the solvent: peaks in the correlation functions are able to persist over longer time ranges in the presence of the solvent, while they are quickly lost in the simulations without the explicit solvent. In contrast, the spatio-temporal correlations for the cluster-forming type-B particles are able to survive both in time and space even in the absence of the solvent.

Acknowledgments

The authors would like to thank Daniele Coslovich (Montpellier) and Lukas Strauss (Wien) for helpful discussions. This work was financially supported by the Austrian Research Fund (FWF) under Proj. Nos P19890-N16 and F41 (SFB ViCoM), the Doktoratskolleg of the Technische Universität Wien ('Computational Materials Science'), by the Marie Curie ITN-COMPLOIDS (Grant Agreement No. 234810), and by the Studienstiftung des Deutschen Volkes.

References

- [1] Mladek B M, Gottwald D, Kahl G, Neumann M and Likos C N 2006 *Phys. Rev. Lett.* **96** 045701
- Mladek B M, Gottwald D, Kahl G, Neumann M and Likos C N 2006 *Phys. Rev. Lett.* **97** 019901(E) (erratum)
- [2] Mladek B M, Charbonneau P and Frenkel D 2007 *Phys. Rev. Lett.* **99** 235702
- [3] Likos C N, Mladek B M, Gottwald D and Kahl G 2007 *J. Chem. Phys.* **126** 224502
- [4] Mladek B M, Gottwald D, Kahl G, Neumann M and Likos C N 2007 *J. Phys. Chem. B* **111** 12799
- [5] Mladek B M, Charbonneau P, Likos C N, Kahl G and Frenkel D 2008 *J. Phys.: Condens. Matter* **20** 494245
- [6] Mladek B M, Kahl G and Likos C N 2008 *Phys. Rev. Lett.* **100** 028301
- [7] Zhang K, Charbonneau P and Mladek B M 2010 *Phys. Rev. Lett.* **105** 245701
- [8] Imperio A and Reatto L 2004 *J. Phys.: Condens. Matter* **16** S3769
- [9] Stradner A, Sedgwick H, Cardinaux F, Poon W C K, Egelhaaf S U and Schurtenberger P 2004 *Nature* **432** 492
- [10] Imperio A and Reatto L 2006 *J. Chem. Phys.* **124** 164712
- [11] Archer A J 2008 *Phys. Rev. E* **78** 031402
- [12] Fragner H 2007 *Phys. Rev. E* **75** 061402
- [13] Cinti F, Jain P, Boninsegni M, Micheli A, Zoller P and Pupillo G 2010 *Phys. Rev. Lett.* **105** 135301
- [14] Saccani S, Moroni S and Boninsegni M 2011 *Phys. Rev. B* **83** 092506
- [15] Coslovich D, Strauss L and Kahl G 2011 *Soft Matter* **7** 2127
- [16] Moreno A J and Likos C N 2007 *Phys. Rev. Lett.* **99** 107801
- [17] Camargo M, Moreno A J and Likos C N 2010 *J. Stat. Mech.* P10015
- [18] Schlesinger M F, Zaslavsky G M and Klafter J 1993 *Nature* **363** 31
- [19] Paul W and Baschnagel J 1999 *Stochastic Processes. From Physics to Finance* (Berlin: Springer)
- [20] Klages R, Radons G and Sokolov I M 2008 *Anomalous Transport* (Wienheim: Wiley-VCH)
- [21] Zaslavsky G M 2002 *Phys. Rep.* **371** 461
- [22] Nägele G and Baur P 1997 *Physica A* **245** 297
- [23] Ripoll M, Mussawisade K, Winkler R G and Gompper G 2004 *Europhys. Lett.* **68** 106
- [24] Malevanets A and Kapral R 1999 *J. Chem. Phys.* **110** 8605–13
- [25] Gompper G, Ihle T, Kroll D M and Winkler R G 2009 *Adv. Polym. Sci.* **221** 1
- [26] Likos C N, Lang A, Watzlawek M and Löwen H 2001 *Phys. Rev. E* **63** 031206
- [27] Ihle T and Kroll D M 2003 *Phys. Rev. E* **67** 066705
- [28] Ihle T and Kroll D M 2001 *Phys. Rev. E* **63** 020201
- [29] Boon J P and Yip S 1992 *Molecular Hydrodynamics* (New York: Dover)
- [30] Hansen J P and McDonald I R 2006 *Theory of Simple Liquids* (New York: Academic)
- [31] Overduin S D and Likos C N 2009 *Europhys. Lett.* **85** 26003
- [32] Overduin S D and Likos C N 2009 *J. Chem. Phys.* **131** 034902